Pages: 26-37 / Vol. 17- No. 2 /Summer- Fall 2024

Journal of Aerospace Science and Technology

Journal Homepage: www:jast.ias.ir

Original Research Article

Investigation of effective parameters on graphite distribution in FGM structure of $A356/Al_2O_3/Gr$ composite

Ali Alizadeh[1]*, Mohsen Heydari Bani, , Jafar Eskandari Jam

1-2-3- Department of Materials and Manufacturing Technologies, Malek Ashtar University of Technology, Tehran, Iran

ABSTRACT

Article History:
Received: 08. January. 2024
Revised: 27. January.2024
Accepted: 27. Fabruary.2024
Available online: 01. October.2024

Keywords: *Aluminum-based composite, FGM structure, centrifugal casting, hybrid composite, graphite, alumina*

DOI :
doi.org/10.22034/jast.2024.430111.1171

In this study, a hybrid aluminum/alumina/graphite composite was prepared using the Horizontal Centrifugal Casting method, and the microstructure and distribution of alumina and graphite particles in the radial direction of the sample cross-sections were investigated. The distribution of graphite and alumina particles resulted in the formation of a Functionally Graded Material (FGM) structure along the cross-section length. Due to the centrifugal force, graphite particles were separated in the inner part of the sample, while alumina particles gradually increased from the inner to the outer region. Samples with 3, 5, and 7% volume fractions of graphite particles added to the melt were obtained using mold rotation speeds of 1000 RPM, 1500 RPM, and 2000 RPM, and the formation of an internal graphite-rich zone was examined. In all samples, a 3% volume fraction of alumina particles was used, and the effect of the presence of alumina particles on the distribution of graphite particles was studied. Optical Microscopy (OM) was used to investigate the microstructure and distribution of graphite and alumina particles. Increasing the amount of graphite from 3 to 7% volume fraction increased the collision and interaction between graphite particles, resulting in a thicker inner graphite-rich layer. Increasing the mold rotation speed initially led to an increase in the thickness of the inner layer and then resulted in a decrease. The presence of alumina particles prevented the complete separation of graphite particles in the inner region and led to a more uniform distribution.

Introduction

A composite material is a combination of two or more distinct and chemically different materials that are insoluble in each other and have a clear common interface [1]. In metal matrix composites, the matrix is a metal and the reinforcement may be another metal or a different material such as ceramic or organic phase. When a composite has more than two types of reinforcements, it is called a hybrid composite [2]. Blending metals with low density with reinforcing particles leads to the production of components with higher performance and functionality that can replace existing homogeneous materials [3]. Aluminum matrix composites are continuously improving due to their low density, high strength, and improved wear resistance [4]. In aluminum matrix composites, the aluminum matrix consists of pure aluminum or aluminum alloys, and the reinforcement used is ceramics such as SiC, $Al2O3$, $SiO2$, $B4C$, etc [5].

Functionally Graded Materials (FGMs) are advanced materials that exhibit a gradual change in microstructure and/or chemical composition in a specific direction. These materials have various applications in the automotive, aerospace, defense, and electronics industries. There are various

1 (Corresponding Author), Ali Alizadeh, Associate Prefosser , Email: **a.alizadeh@mut.ac.ir**

methods for producing gradient materials such as chemical vapor deposition, physical vapor deposition, sol-gel method, plasma spray technique, melt infiltration method, powder metallurgy techniques, centrifugal casting, etc [6,7].

Centrifugal casting is one of the methods for producing gradient materials and is used for mass production of engineering components and parts of large sizes due to its simplicity and lower cost compared to other available methods [8]. This process involves synthesizing a metal matrix composite by centrifugal casting accompanied by centrifugal separation to form a gradual microstructure. When a melt containing particles is subjected to centrifugal force, solid particles are distributed gradiently within the sample volume. The movement of solid particles is determined based on the difference in density between them and the molten metal [9]. Regarding aluminum, the rich zone for heavier particles such as SiC, alumina, and zirconia is the outer region, while for lighter particles like graphite, mica, and carbon micro balloons, it is the inner region [6]. The thickness of the layers and the volume fraction of particles in the two phases are functions of various parameters such as casting temperature, mold rotation speed, melt viscosity, initial volume fraction of particles, particle size, mold temperature, and melt cooling rate [10].

The thickness of the particle-free zone decreases with an increase in the particle volume fraction, while the thickness of the gradient zone increases [11]. Zhao et al. [12] studied the effect of SiC particle volume fraction on the particle distribution in Al-SiC centrifugal casting composites. They reported that an increase in the SiC volume fraction from 5 to 15% led to a decrease in the thickness of the particle-free zone and an increase in the thickness of the particle-rich zone. It has been reported that an increase in the mold rotation speed results in a decrease in the thickness of the particle-rich layer and an increase in the particle volume fraction in this layer [12-14]. Wang et al. [15] investigated the centrifugal casting of Al/SiC composites with a 20% volume fraction of SiC particles and the effect of different mold rotation speeds. They found that SiC particles accumulated in the outer region of the casting piece and observed that with an increase in the mold rotation speed from 600RPM to 800RPM, which signifies an increase in the centrifugal force, the particle volume fraction in the outer region increased, and a sharper gradient of particle volume change was observed.

In this study, the A356 alloy was used as the matrix, and graphite and alumina particles were used as reinforcements. The distribution of graphite and alumina particles on the surface of the samples was investigated, and the effects of the added graphite volume fraction on the melt, mold rotation speed, and the presence of alumina particles on the distribution of graphite particles were studied.

Experimental Method

Raw Materials

The alloy used in this study is A356 aluminum, whose chemical composition is presented in Table 1. Al_2O_3 powder with 99.6% α-phase content and an average particle size of about 60 microns (Figure 1a) from Nabaltek company, and graphite powder with pseudo-spherical particles and an average size of approximately 110 microns was used (Figure b1).

Table 1. Chemical composition of A356 aluminum alloy

Element	Al	Si	Fe	Cu	Mn	Mg	Zn	Ti	Pb
Weight %	balance	7.01	0.15	0.05	<0.03	0.43	<0.03	0.05	<0.01

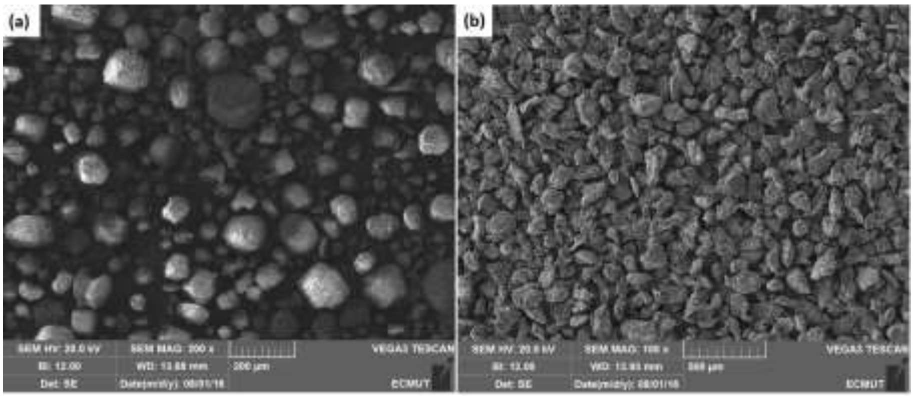

Figure 1. SEM image of (a) Al2O3 and (b) graphite powders.

Fabrication Method

A centrifugal casting method was used to prepare a melt containing alumina and graphite particles. Graphite particles with 3, 5, and 7% volume fractions along with a 3% volume fraction of alumina particles were added to the melt. To improve the attachment of particles to the melt, the powders were placed inside an aluminum foil. Then, they were preheated to 200 degrees Celsius and gradually added to the aluminum melt in several stages. After adding the powders, a mechanical stirrer with a speed of 700 revolutions per minute was used to create turbulence and homogeneously distribute the particles. The stirrer used was made of graphite and had three blades at a 45-degree angle. After 3 minutes of stirring, the melt was poured into the mold of the centrifugal casting machine. The casting temperature was 850 degrees Celsius, and the mold was preheated to 200 degrees Celsius. Different mold rotation speeds of 1000RPM, 1500RPM, and 2000RPM were used to produce the samples. The specifications of the fabricated samples are listed in Table 2. A coding system presented in Table 2 was used to better identify the samples. For example, code 5G3A2000 corresponds to a sample with a 5% volume fraction of graphite and a 3% volume fraction of alumina with a mold rotation speed of 2000 revolutions per minute.

Table 2- Specifications of the cast samples.

Sample No.	Sample Code	Casting Temp. ℃	Alumina %	Graphite %	Mold Rotation Speed (RPM)
1	1000A3G3	850℃	3	3	1000
2	1000A3G5	850℃	3	5	1000
3	1000A3G7	850℃	3	7	1000
4	1500A3G3	850℃	3	3	1500
5	1500A3G5	850℃	3	5	1500
6	1500A3G7	850℃	3	7	1500
7	2000A3G3	850℃	3	3	2000
8	2000A3G5	850℃	3	5	2000
9	2000A3G7	850℃	3	7	2000
10	1500A1	850℃	0	0	1500
11	1500Gr3	850℃	0	5	1500

Microstructural Studies

Optical microscopy was used to investigate the distribution of graphite and alumina particles, the particle sizes in different sample areas, and the microstructure of the samples. For this purpose, sections of the cast samples were cut, polished, and placed under a light microscope. After obtaining images, the Clemex Image Analysis software was used to determine the volume fractions of graphite and alumina particles in different areas of the cross-section and to analyze the particle size distribution in the samples.

Results and Discussion

Particle Distribution Analysis

Figure 2 shows a macroscopic image of the cross-section of the cast sample. As observed, the sample consists of two distinct layers, the inner and outer layers.

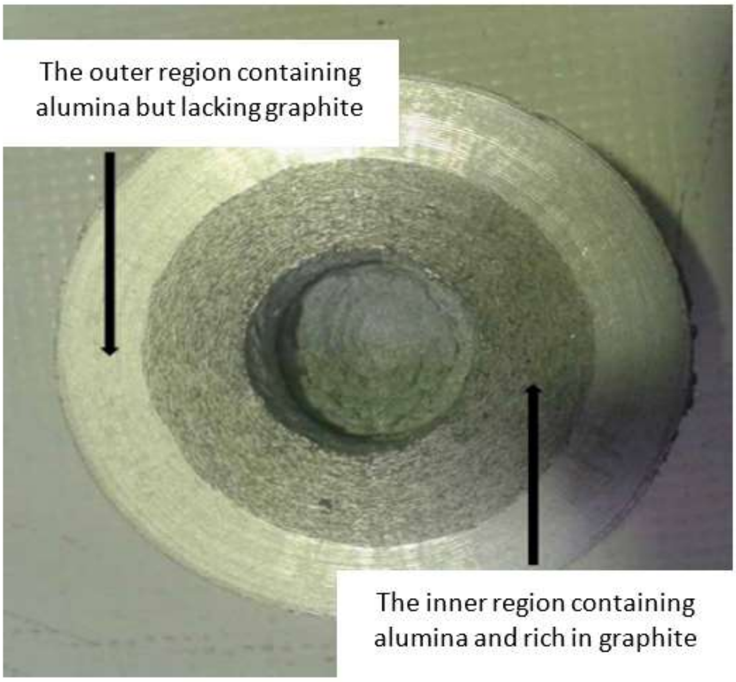

Figure 2. Macroscopic image of the cross-section of the sample.

The inner region contains a high volume fraction of graphite particles along with a low volume fraction of alumina particles. Due to the lower density of graphite compared to the aluminum melt, graphite particles have accumulated in the inner region. Alumina particles are distributed throughout the entire cross-sectional area, gradually increasing from the inner to the outer part, where they have a higher volume fraction. This is due to the higher density of alumina particles compared to the aluminum melt. Figure 3 illustrates microscopically the distribution of graphite particles on the cross-sectional surface.

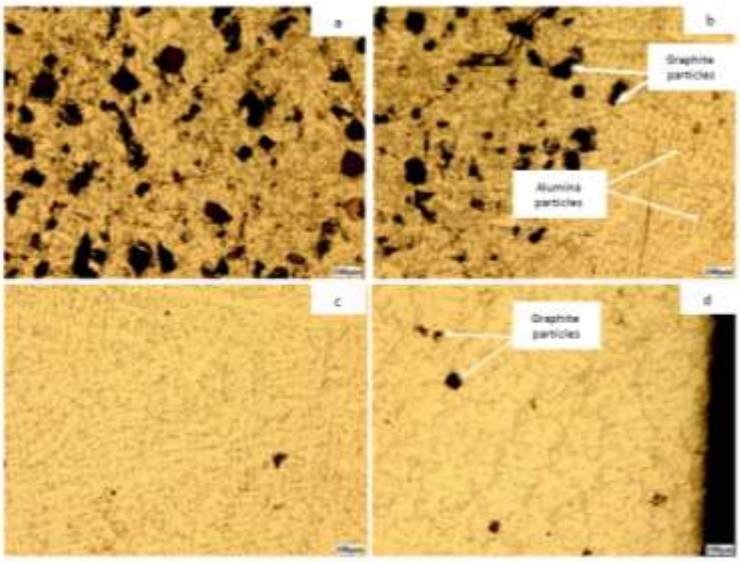

Figure 3. The images of light microscopy show the distribution of graphite particles in the a) internal region, b) boundary between the two internal and external regions, c) graphite-free region, and d) outer edge of the specimen.

From the internal edge of the sample to the boundary between the two internal and external regions, graphite particles are distributed with a gradual decrease in quantity. After that, the amount of graphite particles reaches zero, forming a graphite-free area. As Figure 3-D depicts, a very small number of graphite particles are observed near the outer edge region. Due to the high solidification rate at the outer edge of the sample, which is in contact with the mold, the particles did not have the opportunity to move toward the internal regions and got trapped in this area. Figure 4 shows the distribution chart of graphite particles in this specimen. The large size of the graphite particles caused them to have a high velocity due to the centrifugal force and move toward the inner region. Therefore, in the outer region, a layer free of graphite particles is formed, and the amount of graphite particles in this area reaches zero. It is necessary to mention that on the outer edge of the sample, very low percentages of graphite particles exist due to the high solidification rate

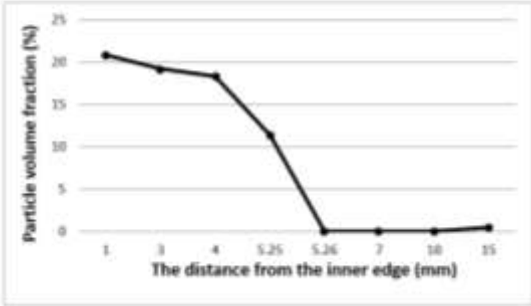

Figure 4. The distribution chart of graphite particles on the sample surface.

Figure 5 provides images of light microscopy showing the distribution of alumina particles in the internal and external regions. As observed, the particles show an appropriate distribution in the external region. Additionally, in the internal region, due to the presence of graphite particles, the alumina particles got trapped and could not move toward the outer region. Figure 6 shows the distribution chart of alumina particles.

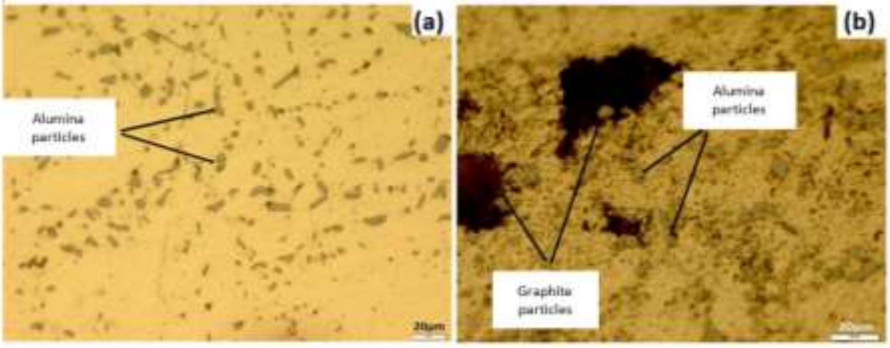

Figure 5. Images of light microscopy showing the distribution of alumina particles (a) in the external region and (b) in the internal region.

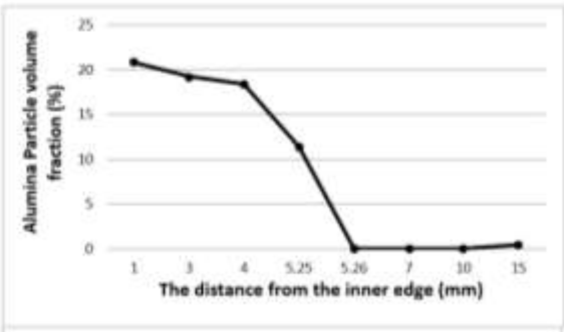

Figure 6. Distribution chart of alumina particles.

Examination of the size of graphite and alumina particles on the sample cross-section

According to Stoke's law, larger particles have a higher velocity in the melt, with the velocity increase of a particle being proportional to the square of its size. Therefore, an increase in particle size leads to a more steep and rapid distribution of particles on the sample surface, with larger particles having a higher tendency to move toward the internal region [16]. Figure 7 shows images of graphite particles in different regions of the inner layer of the sample. As observed, particles closer to the internal edge have a larger diameter compared to those further away.

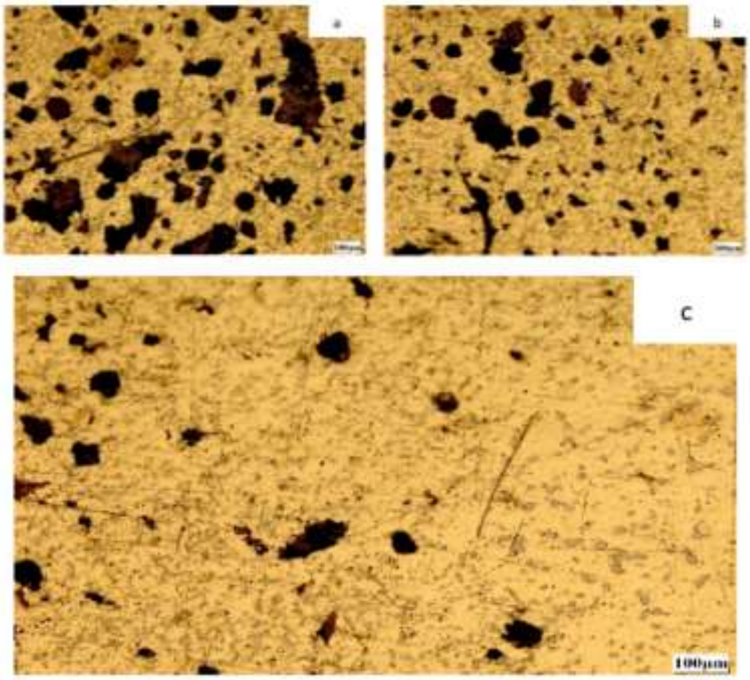

Figure 7. Graphite particles in the sample, 3G3A1000, (a) near the internal edge with an average diameter of 88.92 micrometers, (b) at a distance of 3 mm from the internal edge with an average diameter of 62.63 micrometers, and (c) at a distance of 4.8 mm from the internal edge with an average diameter of 51.39 micrometers.

Figure 8 depicts the average diameter of alumina particles in different regions of the sample 3G3A1000. It is evident that larger particles are more prevalent in the external region and decrease in size as they move towards the internal regions, consistent with the prediction of Stoke's relationship.

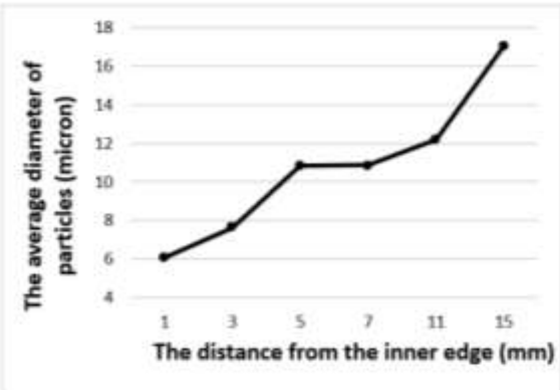

Figure 8. The average diameter of alumina particles in different regions of sample 3G3A1000.

3-3 Investigation of the thickness of the inner particle-enriched layer The thickness of the inner reinforced layer and the volumetric fraction of particles in this layer were measured and analyzed with different percentages of added graphite particles. To assess the thickness of the inner reinforced layer, a criterion called the "particle separation ratio" was utilized. This ratio is defined based on Equation (1).

$$k = a/L \quad (1)$$

where a is the thickness of the reinforced layer and L is the total thickness of the sample. The value of L is almost equal in all samples, but the value of a varies with the rotation speed of the mold and the amount of graphite particles added to the melt. Figure 9 shows the values of a and L on the sample.

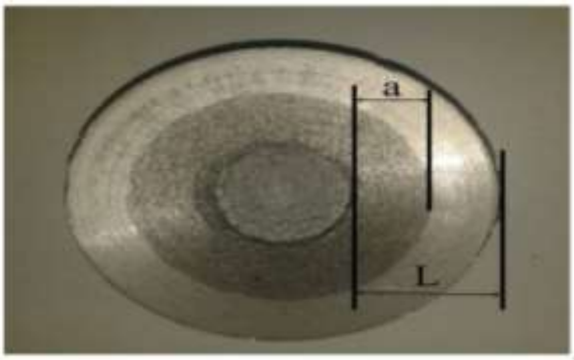

Figure 9. Values of a and L in the sample.

Figure 10 demonstrates the effects of the volumetric fraction of added graphite particles on the thickness of the inner reinforced layer, the value of k, and the volumetric fraction of graphite in the inner layer for different mold rotation speeds. With an increase in the volumetric fraction of added graphite particles, the thickness of the inner layer has increased at each specified speed. The increase in the volumetric fraction of added graphite particles results in more collisions between the particles. As a result, the individual particle velocity in the melt decreases, leading to an increase in the thickness of the graphite-rich inner layer [10]. On the other hand, an increase in the volumetric fraction of particles increases the viscosity of the molten material, reducing the particle mobility. Consequently, the thickness of the particle-enriched layer increases [17].

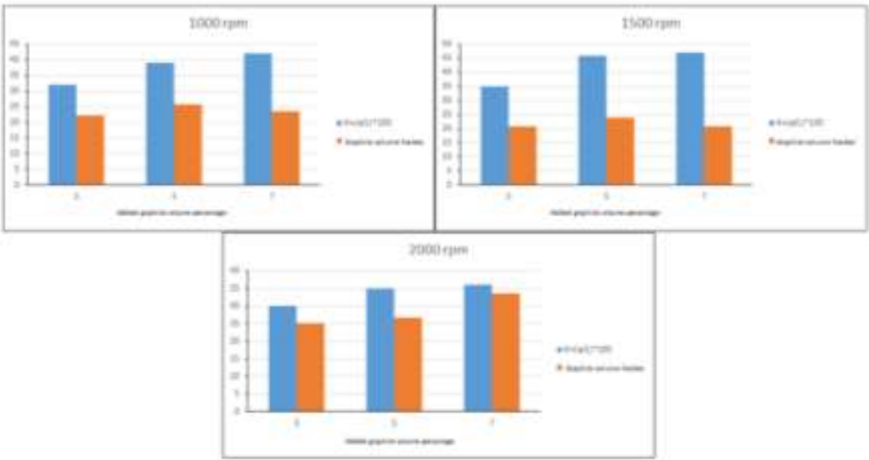

Figure 10. Changes in layer thickness (k) and volumetric fraction of graphite particles with added graphite volume percentage.

Figure 11 illustrates the effect of mold rotation speed on the thickness of the inner layer and the volumetric fraction of graphite particles. With an increase in mold rotation speed from 1000 rpm to rpm1500, the thickness of the reinforced layer increases, and the volumetric fraction of particles decreases. However, with an increase in speed up to 2000 rpm, the thickness of the layer decreases, and the volumetric fraction of particles increases. An increase in mold rotation speed enhances the centrifugal force acting on the particles, increasing their velocity. Moreover, it raises the heat transfer coefficient, increasing the solidification rate. Therefore, mold rotation speed has two opposing effects on particle movement and controls the thickness of the particle-enriched layer [10].

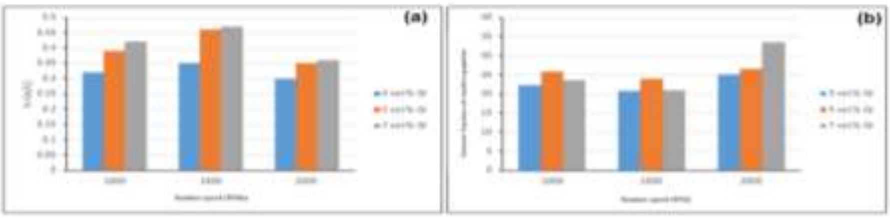

Figure 11. Influence of rotation speed on (a) layer thickness (K) and (b) volumetric fraction of graphite particles.

At a rotational speed of 1500 RPM, it can be said that the particles are influenced by the solidification rate and cannot reach the inner region. The fast movement of the solidification front and the low speed of the particles compared to the solidification front speed leads to the entrapment of particles in the intermediate regions, resulting in an increase in the thickness of the inner layer. In samples cast at a rotational speed of 1000 RPM, the rotational speed is not high enough to significantly increase the solidification rate and trap the particles, preventing their free movement toward the inner regions. On the other hand, the rotational speed is enough to quickly move the particles and overcome the solidification rate, resulting in the separation of particles in the inner layer. Therefore, the thickness of the graphite-rich layer decreases. At a rotational speed of RPM2000, the solidification rate increases, and the trapped particles in the sample also increase. However, the particles in the intermediate regions of the sample, due to the high mold rotational speed, acquire high speed and reach the inner regions. In summary, in this case, the particle velocity is greater than the solidification rate. The centrifugal force, G, can be obtained using equation 2. The centrifugal force, G, generated at a rotational speed of 2000 RPM is 223/57, and at a rotational speed of 1000 RPM, it is 55.89. The centrifugal force acting on the particles at a rotational speed of 2000 RPM is higher, therefore, the inner layer thickness for samples with a rotational speed of 2000 RPM is the lowest.

$$G=\frac{\omega^2 r}{g} \tag{2}$$

Investigation of the effect of the presence of alumina particles on the distribution of graphite particles

Alumina particles, due to their higher density than the melt, tend to move towards the outer regions. Because their movement is opposite to the movement of graphite particles, they collide with graphite particles and prevent the free movement of graphite particles towards the inner regions. Therefore, graphite particles cannot completely reach the inner regions, and as a result, their volumetric fraction in the reinforced layer is also affected. Figure 12 shows the collision of alumina particles with graphite particles.

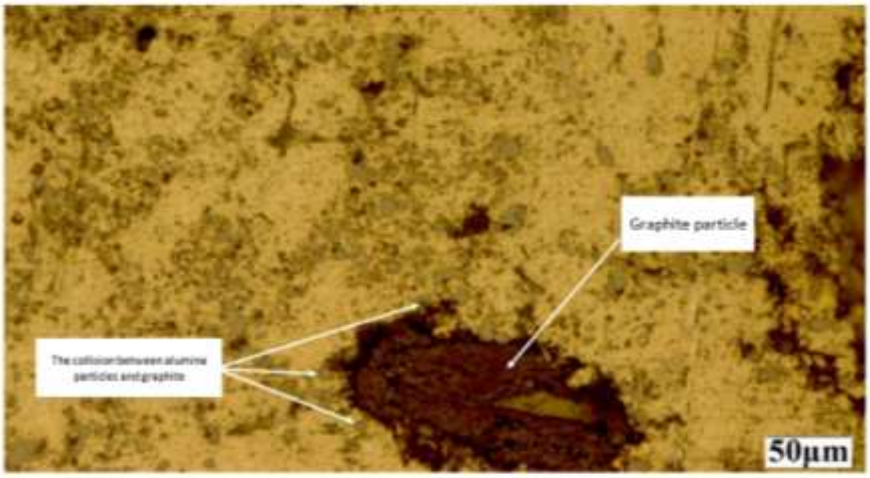

Figure 12. The collision of alumina particles with graphite particles.

According to the Stokes equation, equation (3), particles with a larger size have a higher velocity in the melt. The study of the effect of the size of graphite and alumina particles shows that graphite particles have a velocity approximately 65 times higher than alumina particles.

$$V=\frac{|\rho_p-\rho_m|\, Gg\, D_p^2}{18\eta} \tag{3}$$

For graphite particles with an average diameter of 110 microns and a density of 2 g/cm^3;

$$V_{Gr}=470Gg/\eta \tag{4}$$

For alumina particles with an average diameter of 10 microns and a density of 3.95 g/cm^3;

$$V_{Alumina}=7.2Gg/\eta \tag{5}$$

Resulting in;

$$\frac{V_{Gr}}{V_{Alumina}}= \ 65\,\frac{470Gg/\eta}{7.2Gg/\eta} \tag{6}$$

The higher velocity of graphite particles allows them to act more effectively when colliding with alumina particles and prevents them from being significantly influenced by alumina particles. Therefore, alumina particles, while affecting the accumulation of graphite particles in the inner layer, cannot pull graphite particles toward the outer regions and prevent the separation of graphite particles in the inner layer. Thus, graphite particles, in the presence of alumina particles, are also concentrated with a clear boundary in the inner layer, and these alumina particles become trapped under the influence of graphite particles in the inner layer and unable to move towards the outer layer. To investigate the effect of the presence of alumina particles on the movement of graphite particles, the volumetric fraction diagram of sample 1500G3 was compared with sample 1500A3G5. This diagram is shown in Figure 11. The mold rotational speed and the percentage of added graphite particles were constant in both samples, with values of 1500 RPM and five volume percent, respectively, with the difference that sample 1500A3G5 contained alumina particles, while sample 1500G3 did not. The comparison of these two samples indicates the effect of alumina particles on the movement of graphite particles.

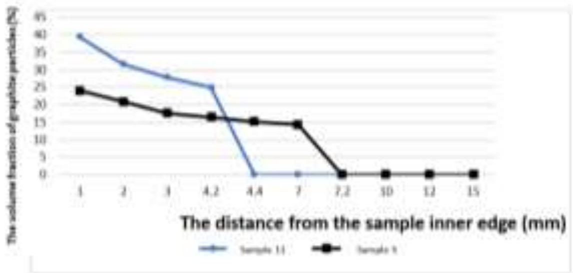

Figure 13. The comparison chart of graphite particle distribution for samples 5 and 11.

As shown in Figure 13, the absence of alumina particles facilitates the movement of graphite particles toward the inner regions, resulting in a decrease in the k ratio and an increase in the volumetric fraction of graphite particles in the inner layer. The alumina particles present in the melt increase the melt viscosity and prevent the complete accumulation of graphite particles in the inner region due to collisions with graphite particles.

Conclusion

The present study investigated the effective parameters on the distribution of graphite in the FGM composite structure A356/Al2O3/Gr. The results indicate that: in samples cast at a rotational speed of 1000 RPM, the solidification rate is low and does not prevent the free movement of particles. However, the particles have the necessary speed for movement and therefore, their speed overcomes the solidification rate, pulling the particles towards the inner regions. At a rotational speed of RPM2000, the solidification rate increases, and trapped particles at the two ends of the sample also increase. However, the particles present in the intermediate regions of the sample acquire high speed due to the high rotational speed of the mold, reaching the inner regions. In summary, in this case as well, the particle velocity is greater than the solidification rate. Due to the centrifugal force at a rotational speed of 2000 RPM being significantly higher than at 1000 RPM, the inner layer thickness is lower at a rotational speed of 2000 RPM. At a rotational speed of 1500 RPM, it can be said that the particles are influenced by the solidification rate and cannot reach the inner region. In fact, there is an equilibrium between the solidification rate and the particle velocity, and one factor does not dominate over the other. This leads to an increase in the thickness of the inner layer. Graphite particles, due to their large size, are separated with a clear boundary in the inner region, while the fine alumina particles are distributed smoothly over the entire cross-section of the sample. The sample was divided into two inner layers containing graphite and alumina particles and an outer layer containing alumina particles without graphite particles.

References

1. ASM HandBook Volume 21-Composites. 2001.
2. Menezes, P.L., P.K. Rohatgi, and M.R. Lovell, Self-Lubricating Behavior of Graphite Reinforced Metal Matrix Composites, in Green Tribology: Biomimetics, Energy Conservation and Sustainability, M. Nosonovsky and B. Bhushan, Editors. 2012, Springer Berlin Heidelberg: Berlin, Heidelberg. p. 445-480.
3. Thirumalai, T., et al., Production and characterization of hybrid aluminum matrix composites reinforced with boron carbide (B4C) and graphite. Journal of Scientific & Industrial Research, 2014. **Vol.73**: p. 667-670.
4. Gewfiel, E., M.A.H. El-Meniawi, and Y. Fouad, The effects of graphite and SiC formation on mechanical and wear properties of aluminum-graphite (Al/Gr) composites, in 2012 International Conference on Engineering and Technology (ICET). 2012, Institute of Electrical & Electronics Engineers (IEEE).
5. Kala, H., K.K.S. Mer, and S. Kumar, A Review on Mechanical and Tribological Behaviors of Stir Cast Aluminum Matrix Composites. Procedia Materials Science, 2014. p. **6:** 1951-1960.
6. Rajan, T.P.D. and B.C. Pai, Processing of Functionally Graded Aluminium Matrix Composites by Centrifugal Casting Technique. Materials Science Forum, 2011. **690**: p. 157-161.

7. El-Hadad, S., et al., Fabrication of Al-Al3Ti/Ti3Al Functionally Graded Materials under a Centrifugal Force. Materials, 2010. **3**(9): p. 4639-4656.

8. Rajan, T.P.D., R.M. Pillai, and B.C. Pai, Centrifugal casting of functionally graded aluminium matrix composite components. International Journal of Cast Metals Research, 2008. **21**(1-4): p. 214-218.

9. Wang, K., et al., An approach for increase of reinforcement content in particle rich zone of centrifugally cast SiCP/Al composites. Journal of Composite Materials, 2012. **46**(9): p. 1021-1027.

10. Kim, J.K. and P.K. Rohatgi, Formation of a graphite-rich zone in centrifugally cast copper alloy graphite composites. Journal of Materials Science, 1998. **33**(8): p. 2039-2045.

11. Bonollo, F., et al., Cilinder liners in aluminium matrix composite by centrifugal casting. La metallurgia italiana, 2004(6).

12. Gao, J. and C. Wang, Modeling the solidification of functionally graded materials by centrifugal casting. Materials Science and Engineering: A, 2000. **292**(2): p. 207-215.

13. El Hadad, S., H. Sato, and Y. Watanabe. Investigation of the mechanical properties in Al/Al3Zr FGMs fabricated by centrifugal casting method. in Materials Science Forum. 2010. Trans Tech Publ.

14. Watanabe, Y., N. Yamanaka, and Y. Fukui, Control of composition gradient in a metal-ceramic functionally graded material manufactured by the centrifugal method. Composites Part A: Applied Science and Manufacturing, 1998. **29**(5): p. 595-601.

15. Wang, K., et al., Microstructures in centrifugal casting of SiCp/AlSi9Mg composites with different mould rotation speeds. J. Wuhan Univ. Technol.-Mat. Sci. Edit., 2011. **26**(3): p. 504-509.

16. Velhinho, A., et al. Al/SiCp functionally graded metal-matrix composites produced by centrifugal casting: Effect of particle grain size on reinforcement distribution. in Materials Science Forum. 2003. Aedermannsdorf, Switzerland: Trans Tech Publications, 1984.-

17. Panda, E., S.P. Mehrotra, and D. Mazumdar, Mathematical modeling of particle segregation during centrifugal casting of metal matrix composites. Metallurgical and Materials Transactions A, 2006. **37**(5): p. 1675-1687.

HOW TO CITE THIS ARTICLE:

Ali Alizadeh, Mohsen Heydari Bani, Jafar Eskandari Jam, "Investigation of effective parameters on graphite distribution in FGM structure of A356/Al_2O_3/Gr composite", **Journal of Aerospace Sciece and Technology**, **Vol 17, No**2, **2024, pp,** 26-37
DOI: doi.org/10.22034/jast.2024.430111.1171
URL: https://jast.ias.ir/article_188628.html